Ferromagnetic Kondo-lattice model

2003 J. Phys. A: Math. Gen. 36 9275

(http://iopscience.iop.org/0305-4470/36/35/313)

INSTITUTE OF PHYSICS PUBLISHING JOURNAL OF PHYSICS A: MATHEMATICAL AND GENERAL

J. Phys. A: Math. Gen. **36** (2003) 9275–9288 PII: S0305-4470(03)59814-6

Ferromagnetic Kondo-lattice model

W Nolting, W Müller and C Santos

Lehrstuhl Festkörpertheorie, Institut für Physik, Humboldt-Universität zu Berlin, Invalidenstraße 110, 10115 Berlin, Germany

Received 19 February 2003, in final form 3 April 2003
Published 20 August 2003
Online at stacks.iop.org/JPhysA/36/9275

Abstract

We present a many-body approach to the electronic and magnetic properties of the (multiband) Kondo-lattice model with ferromagnetic interband exchange. The coupling between itinerant conduction electrons and localized magnetic moments leads, on the one hand, to a distinct temperature dependence of the electronic quasiparticle spectrum and, on the other hand, to magnetic properties such as, e.g., the Curie temperature T_C or the magnon dispersion, which are strongly influenced by the band electron self-energy and therewith in particular by the carrier density. We present results for the single-band Kondo-lattice model in terms of quasiparticle densities of states and quasiparticle band structures and demonstrate the density dependence of the self-consistently derived Curie temperature. The transition from weak-coupling (RKKY) to strong-coupling (double exchange) behaviour is worked out. The multiband model is combined with a tight-binding-LMTO band structure calculation to describe real magnetic materials. As an example we present results for the archetypal ferromagnetic local-moment systems EuO and EuS. The proposed method avoids the double counting of relevant interactions and takes into account the correct symmetry of atomic orbitals.

PACS numbers: 75.30.Mb, 75.50.−y

1. Introduction

The Kondo-lattice model (KLM), also denoted as the *s*–*f* or *s*–*d model* or, in its strong-coupling regime, as the *double exchange model*, is today surely one of the most prominent models in solid state theory, and that is mainly because of its great variety of important applications to rather hot topics in the wide field of collective magnetism. It refers to magnetic materials which get their magnetic properties from a system of localized magnetic moments being indirectly coupled via an interband exchange J to itinerant conduction electrons. Many characteristic properties of such materials can be traced back to this interband exchange.

There are a lot of important applications of the KLM, first of all to the classical systems of magnetic semiconductors such as EuO and EuS [1] and magnetic metals such as Gd [2]

($J > 0$, weak to intermediate coupling). All these materials have strictly localized moments because of the half-filled 4f shell of the rare earth ion (Eu^{2+}, Gd^{3+}). The striking temperature dependence of the unoccupied (!) conduction band states in the EuX [1] manifesting itself, e.g., in the well-known *redshift effect* [1], and the effective moment coupling in Gd via a conduction electron spin polarization (RKKY) [2] can be understood only by the existence of the interband exchange J.

Other candidates are the intensively investigated diluted magnetic semiconductors such as $Ga_{1-x}Mn_xAs$ with probably negative J (strong coupling). The Mn^{2+} ion creates simultaneously an $S = \frac{5}{2}$ spin and an itinerant hole in the GaAs valence band [3]. The latter takes care of an indirect coupling between the randomly distributed magnetic moments which leads already for very small x to a ferromagnetic order with a maximum T_C of 110 K for $x = 0.053$ [4].

Another hot topic because of the great potential for engineering applications is the colossal magnetoresistance (CMR) materials [5] such as $La_{1-x}(Ca,Sr)_xMnO_3$ which show a very rich magnetic phase diagram. For $0.2 \leqslant x \leqslant 0.4$ the originally antiferromagnetic and insulating parent compound $LaMnO_3$ changes into a ferromagnetic metal. This is ascribed to a homogeneous valence mixing $\left(Mn^{3+}_{1-x}Mn^{4+}_{x}\right)$. The three $3d_{t_{2g}}$ electrons in Mn^{3+} are considered more or less localized forming an $S = \frac{3}{2}$ moment while the additional $3d_{e_g}$ electron is itinerant. Again, the local moment-itinerant electron exchange is made responsible for many typical features of the CMR materials ($J > 0$, strong coupling).

We derive in the next section the multiband Hamiltonian of the Kondo-lattice model which is combined in section 4 with an *ab initio* band structure calculation to get the temperature-dependent electronic structure of the prototype ferromagnets EuO and EuS. To understand the physics of the KLM we present in section 3 for the nondegenerate case an analysis of the magnetic and electronic model properties.

2. Multiband Kondo-lattice model

The system under consideration consists of quasi-free electrons in rather broad conduction bands (d bands) and localized electrons with extremely flat dispersions (f levels). While there is no contribution of the f electrons to the kinetic energy, the part of the d electrons reads

$$H_{\mathrm{d}} = \sum_{ijm\bar{m}\sigma} T_{ij}^{m\bar{m}} c_{im\sigma}^{+} c_{j\bar{m}\sigma}. \tag{1}$$

The hopping process from site $\mathbf{R}_i$ to site $\mathbf{R}_j$ may be accompanied by an orbital change ($m \to \bar{m}$). $T_{ij}^{m\bar{m}}$ are the respective hopping integrals. $c_{jm\sigma}^{+}$ ($c_{jm\sigma}$) is the creation (annihilation) operator for a Wannier electron at site $\mathbf{R}_j$ in the orbital m with spin σ ($\sigma = \uparrow, \downarrow$).

When applying the model study to real local-moment materials, intended as our final goal, we require that the single-electron energies not only account for the kinetic energy and the influence of the lattice potential, but also for all those interactions which are not explicitly covered by the model Hamiltonian. This means that the hopping integrals are to be taken from a proper *ab initio* band calculation. We exemplify the procedure in section 4 for the special case of the ferromagnetic europium chalcogenides. In particular, we show how to avoid the well-known double-counting problem of important interactions.

The Coulomb interaction is restricted to intra-atomic terms. Furthermore, we assume that only two subbands are involved in the scattering process. Then the interaction part can be written as [6]

$$H_c = H_{\mathrm{dd}} + H_{\mathrm{ff}} + H_{\mathrm{df}}. \tag{2}$$

In an obvious manner the Coulomb interaction may be split into three different parts depending on whether both interacting particles stem from a conduction band $H_{\rm dd}$, or both from a flat band $H_{\rm ff}$, or one from a flat band and the other from a conduction band $H_{\rm df}$. The first term refers to electron correlations in the conduction bands, not explicitly taken into account by the KLM. As mentioned, our procedure for describing real materials accounts for such correlations by a proper renormalization of the single-particle energies.

The term $H_{\rm ff}$ describes interactions between electrons from the flat bands which interest us only with respect to the fact that they form permanent magnetic moments (spins),

$$\mathbf{S}_i = \sum_f \boldsymbol{\sigma}_f \tag{3}$$

where $\boldsymbol{\sigma}_f$ is the spin operator of an electron in subband f. If it is necessary to consider a (super)exchange interaction between the local spins then $H_{\rm ff}$ is chosen to be a Heisenberg Hamiltonian, possibly with a symmetry-breaking single-ion anisotropy D:

$$H_{\rm ff} = -\sum_{ij} J_{ij}\mathbf{S}_i \cdot \mathbf{S}_j - D\sum_i \left(S_i^z\right)^2. \tag{4}$$

The third term in (2) $H_{\rm df}$ refers to the interaction between a localized and an itinerant electron. Neglecting unimportant spin-independent contributions it can be written as an intra-atomic exchange, i.e. a local interaction between the conduction electron spin $\boldsymbol{\sigma}_{jm}$ and the local moment spin $\mathbf{S}_j$ [6]:

$$H_{\rm df} = -J\sum_{jm} \boldsymbol{\sigma}_{jm} \cdot \mathbf{S}_j. \tag{5}$$

Here m denotes the conduction electron orbital. J is the exchange coupling constant, assumed to be identical for all df pairs. Using second quantization for the itinerant electron spin $\left(n_{jm\sigma} = c^+_{jm\sigma}c_{jm\sigma}\right)$, this interaction reads

$$H_{\rm df} = -\frac{1}{2}J\sum_{jm}\left(S_j^z(n_{jm\uparrow} - n_{jm\downarrow}) + S_j^+ c^+_{jm\downarrow}c_{jm\uparrow} + S_j^- c^+_{jm\uparrow}c_{jm\downarrow}\right). \tag{6}$$

We see that the first term describes an Ising-like interaction of the two spin operators while the other two provide spin exchange processes between the localized moment and the itinerant electron. In particular, the two latter terms are responsible for many typical properties of the Kondo-lattice materials. Spin exchange may happen in three different elementary processes: magnon emission by an itinerant $\downarrow$ electron, magnon absorption by an $\uparrow$ electron and formation of a quasiparticle (*magnetic polaron*). The latter can be understood as a propagating electron dressed by a virtual cloud of repeatedly emitted and reabsorbed magnons corresponding to a depolarization of the immediate localized spin neighbourhood.

The total Hamiltonian of the multiband Kondo lattice is composed of (1), (2) and (6)

$$H = H_{\rm d} + H_{\rm ff} + H_{\rm df}. \tag{7}$$

An important model parameter is of course the effective coupling constant $\frac{J}{W}$ where W is the Bloch bandwidth. Especially the sign of J is decisive. Other parameters are the local spin S, the lattice structure and above all the band occupation $n = \sum_{m\sigma}\langle n_{m\sigma}\rangle$. In the case of a nondegenerate band n is a number between 0 and 2.

3. Magnetic and electronic model properties

The many-body problem of the KLM is not exactly solvable for the general case even for the nondegenerate case, for which we can remove the orbital dependence and which shall

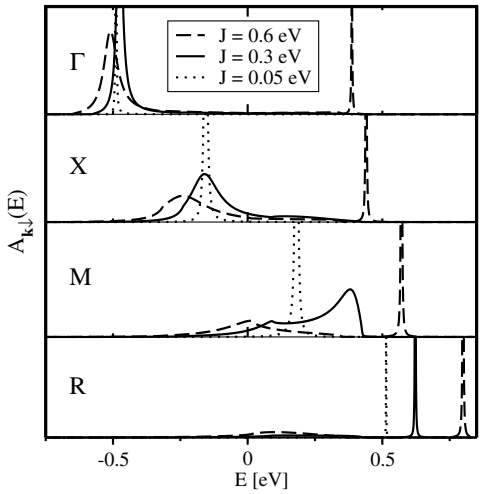

Figure 1. ↓-spectral density as a function of energy for several symmetry points in the first Brillouin zone and for different exchange couplings J. Parameters: $S = \frac{1}{2}$, $W = 1$ eV, sc lattice.

exclusively be tackled in this section:

$$H = \sum_{ij\sigma} T_{ij} c^{+}_{i\sigma} c_{j\sigma} - J \sum_{j} \mathbf{S}_j \cdot \boldsymbol{\sigma}_j = H_0 + H_1. \tag{8}$$

However, there exists a non-trivial, very illustrative limiting case which is rigorously tractable and nevertheless exhibits all the above-mentioned elementary excitation processes [7–10]. It refers to a single electron in an otherwise empty conduction band coupled to a ferromagnetically saturated moment system, e.g. EuO at $T = 0$. In this case the ↑ spectrum is simple, because the ↑ electron cannot exchange its spin with the parallel aligned spin system. Only the Ising-type interaction in (5) and (6) takes care of a rigid shift of the total spectrum by $-\frac{1}{2}JS$. The spectral density is a δ-function at $\epsilon(\mathbf{k}) - \frac{1}{2}JS$ where ϵ is the free Bloch energy, the Fourier transform of the hopping integral T_{ij}. Real correlation effects appear, however, in the ↓ spectrum. Figure 1 shows the energy dependence of the ↓-spectral density for some symmetry points. For weak couplings the spectral density consists of a single pronounced peak. The finite width points to a finite quasiparticle lifetime due to first spin-flip processes, but the quasiparticle band structure, read off from the peak positions, is still very similar in shape to the Bloch dispersion.

This changes drastically already for rather moderate effective exchange couplings JS/W. One observes in certain parts of the Brillouin zone, for a strongly coupled system even in the whole Brillouin zone, that the excitation energy splits into two parts. The sharp high-energy peak belongs to the magnetic polaron while the broader low-energy part consists of scattering states due to magnon emission. As long as the polaron peak is above the scattering spectrum the quasiparticle has even an infinite lifetime. The scattering spectrum is in general rather broad because the emitted magnon can carry away any wave vector from the first Brillouin zone. Because of the concomitant spin-flip, magnon emission can happen only if there are ↑ states within reach. Therefore, the scattering part extends just over that energy region where $\rho_\uparrow \neq 0$ (ρ_σ: quasiparticle density of states (Q-DOS)).

For the general case (finite temperature, finite band occupation) the many-body problem of the KLM cannot be solved exactly. Approximations must be tolerated. The central quantity is the self-energy, for which we use the Green function procedure developed in [11].

This non-perturbational theory can be considered a *moment conserving decoupling approximation* (MCDA) which interpolates between exact limiting cases such as, e.g., the above-discussed example. In more detail, the method decouples the hierarchy of equations of motion by expressing certain 'higher' Green functions as linear combination of 'lower' functions, already involved in the procedure. The ansatz is motivated by exact special cases such as the atomic limit, ferromagnetic saturation, local spin $S = \frac{1}{2}$, full or empty band and so on. Free parameters in the ansatz are eventually fitted to rigorous spectral moments. As other methods too, e.g. the interpolating self-energy approaches in [12, 13], it leads to the following structure of the self-energy:

$$\Sigma_{\mathbf{k}\sigma}(E) = -\tfrac{1}{2} J z_\sigma \langle S^z \rangle + J^2 D_{\mathbf{k}\sigma}(E). \tag{9}$$

Restriction to the first term, only, yields the mean-field approach to the KLM, which is correct for sufficiently weak couplings J. It is due to the Ising part in equation (5) ($z_\sigma = \delta_{\sigma\uparrow} - \delta_{\sigma\downarrow}$). Without the second part of the self-energy it would give rise to a spin-polarized splitting of the conduction band. The term $D_{\mathbf{k}\sigma}(E)$ is more complicated, being predominantly determined by the spin exchange processes. It is a complicated functional of the self-energy itself, i.e. (9) is an implicit equation for $\Sigma_{\mathbf{k}\sigma}(E)$ and not at all an analytical solution. $D_{\mathbf{k}\sigma}(E)$ depends, further on, on mixed spin correlations such as $\langle S_i^z n_{i\sigma} \rangle, \langle S_i^+ c_{i\downarrow}^+ c_{i\uparrow} \rangle, \ldots$, built up by combinations of localized-spin and itinerant-electron operators. Fortunately, all these mixed correlations can rigorously be expressed via the spectral theorem by any of the Green functions involved in the hierarchy of the MCDA.

However, there are also pure local-moment correlations of the form $\langle S_i^z \rangle, \langle S_i^\pm S_i^\mp \rangle$, $\langle (S_i^z)^3 \rangle, \ldots$, which also have to be expressed by the self-energy (9). For this purpose, we use the *modified* RKKY theory of [14] which exploits a mapping of the interband exchange (5) to an effective Heisenberg model,

$$H_{\mathrm{f}} = -\sum_{ij} \hat{J}_{ij} \mathbf{S}_i \cdot \mathbf{S}_j \tag{10}$$

by averaging out the conduction electron degrees of freedom:

$$-J \sum_j \mathbf{S}_j \cdot \boldsymbol{\sigma}_j \longrightarrow -J \sum_j \mathbf{S}_j \cdot \langle \boldsymbol{\sigma}_j \rangle^{(c)} \longrightarrow H_{\mathrm{f}}. \tag{11}$$

In the last analysis this means determining the expectation value $\langle c_{\mathbf{k}+\mathbf{q}\sigma}^+ c_{\mathbf{k}\sigma'} \rangle^{(c)}$. We use again a Green function procedure [14] which eventually leads to effective exchange integrals in (10),

$$\hat{J}_{ij} = \frac{J^2}{4\pi N^2} \sum_{\mathbf{k}\mathbf{q}\sigma} \mathrm{e}^{\mathrm{i}\mathbf{q}\cdot(\mathbf{R}_i - \mathbf{R}_j)} \times \int_{-\infty}^{+\infty} \mathrm{d}E \; f_-(E) \, \mathrm{Im}[(E - \epsilon(\mathbf{k}) + \mathrm{i}0^+)(E - \epsilon(\mathbf{k}+\mathbf{q}) - \Sigma_{\mathbf{k}+\mathbf{q}\sigma}(E))]^{-1} \tag{12}$$

where $f_-(E)$ denotes the Fermi function. The effective exchange integrals are decisively influenced by the conduction electron self-energy Σ_σ which brings a distinct band occupation and temperature dependence to the $\hat{J}_{ij}$. Neglecting Σ_σ leads to the 'conventional' RKKY formula with $J_{ij} \propto J^2$ as a result of second-order perturbation theory. Via Σ_σ higher order terms of the electron spin polarization enter the *modified* RKKY being therefore not restricted to weak couplings only. Note that on the right-hand side of equation (12) the product of two propagators appears. From the equation of motion method in [14] it follows directly that one of them is dressed by a self-energy, the other not.

To get from the effective operator (10) the magnetic properties of the KLM we apply the standard Tyablikov approximation which is known to yield convincing results in the

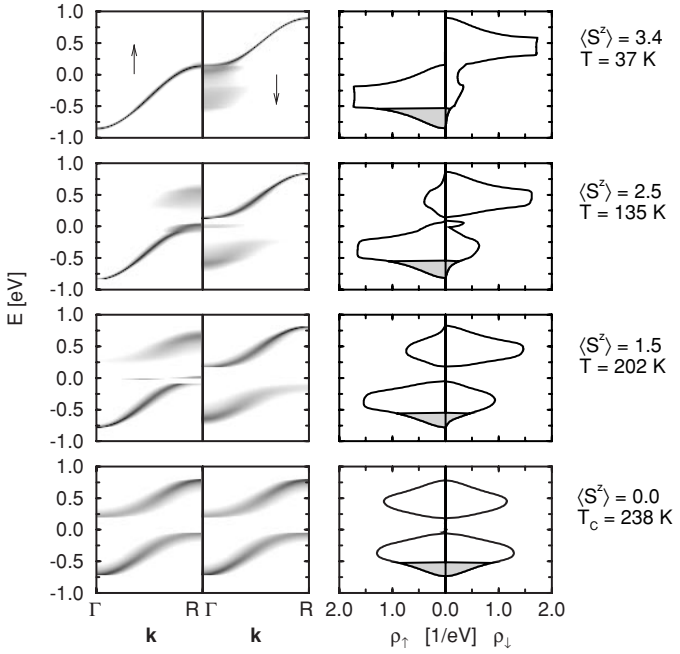

Figure 2. Quasiparticle band structure as a function of wave vector (left column) and quasiparticle density of states as a function of energy (right column) for four different temperatures calculated within the MCDA [11]. Parameters: $J = 0.2\,\mathrm{eV}$, $W = 1\,\mathrm{eV}$, $n = 0.2$, $S = \frac{7}{2}$, sc lattice.

low- as well as in the high-temperature region [14]. All the above-mentioned local-moment correlations are then expressed by the electronic self-energy. We therefore end up with a closed system of equations that can be solved self-consistently for all entities of interest.

Figure 2 shows the temperature dependence of the quasiparticle band structure (Q-BS), derived as a density plot from the spectral density, and the Q-DOS $\rho_\sigma(E)$ for a typical parameter set from the moderate coupling regime ($J = 0.2$ eV, $W = 1\,\mathrm{eV}$, $n = 0.2$, $S = \frac{7}{2}$, sc lattice). In this case, the self-consistently calculated Curie temperature T_C amounts to 238 K. At $T = 37\,\mathrm{K}$ the local-moment magnetization is 3.4 and therewith very close to saturation. The theory reproduces, in spite of the finite carrier concentration, the same features as for the exact ($n = 0$, $T = 0$) case exhibited in figure 1. The $\uparrow$ dispersion as well as the Q-DOS $\rho_\uparrow$ are practically identical to the respective 'free' Bloch functions. The $\downarrow$ spectrum, however, is more complicated. The scattering states take away a substantial part of the spectral weight near the Γ-point while near the R-point the polaron state clearly dominates. With increasing temperature (decreasing $\langle S^z \rangle$) a finite magnon density appears to allow for scattering states in the $\uparrow$ spectrum, too, because of magnon absorption and simultaneous spin-flip by the $\uparrow$ electron. Furthermore, polaron and scattering states separate, where, surprisingly, the rather broad scattering spectrum is in wide wave vector regions bunched to a prominent peak. At $T = T_\mathrm{C}$ the spin asymmetry is removed but there remains a correlation-caused splitting of the spectrum into two branches and two subbands, respectively, due to the interband exchange coupling J. Because of the possibility of mutual spin exchange $\rho_\uparrow$ and $\rho_\downarrow$ occupy for finite temperatures always the same energy regions.

The key quantity of ferromagnetism is the Curie temperature T_C. A finite T_C comes out as a consequence of an indirect coupling between the local moments, mediated by

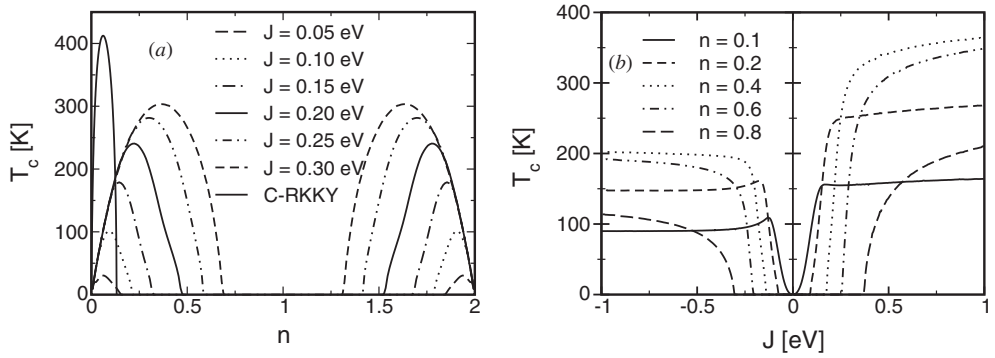

Figure 3. Curie temperature as a function of (*a*) the band occupation n for various J, (*b*) the interband exchange coupling J for various n, calculated by using the *modified* RKKY.

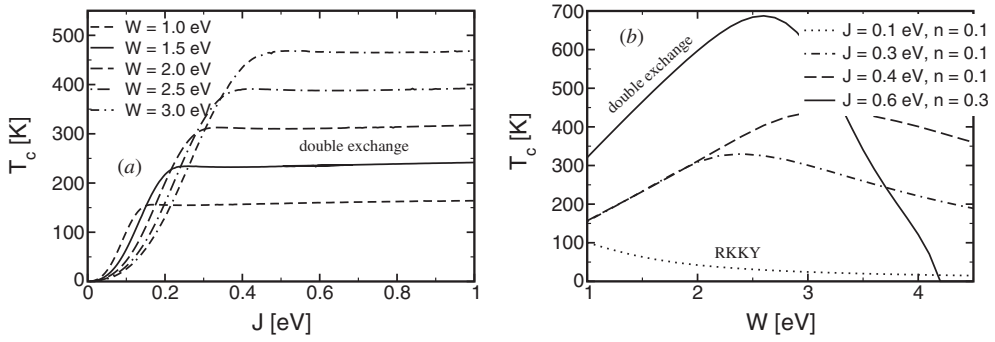

Figure 4. Curie temperature as a function of (*a*) the interband exchange J for various W and $n = 0.1$, (*b*) the Bloch bandwidth W for various J and n, calculated by using the *modified* RKKY.

a polarization of the conduction electron spins. Therefore, T_C exhibits a strong carrier-concentration dependence which is plotted in figure 3. The effective exchange integrals have been taken into account up to 25th neighbours. Ferromagnetism appears for low electron (hole) concentrations, while being excluded in the region around half-filling ($n = 1$). Around $n = 1$ we expect an antiferromagnetic phase, however, not explicitly calculated here. A similar n-dependence of T_C has been found in [17]. It is interesting to compare the results with those of the *conventional* RKKY, given by $\Sigma_\sigma \equiv 0$ in equation (12). A corresponding curve is inserted in figure 3. The maximal T_C values are higher, but ferromagnetism exists only in a very narrow region of low electron (hole) concentrations where this region turns out to be independent of J.

Two features dominate the J-dependence of the Curie temperature plotted in figure 3(*b*). The first is the appearance of a critical J for band occupations for which the *conventional* RKKY does not allow ferromagnetism ($n \geqslant 0.13$). This is in accordance with the fact that for $J \to 0$ the *modified* RKKY reproduces the *conventional* RKKY. The second fact is that T_C runs into a saturation for strong couplings J, where the saturation value depends on the band occupation n. These results are far beyond *conventional* RKKY which can work of course only in the weak coupling regime.

It is interesting to observe (see figure 4) that in the weak coupling RKKY *region* T_C scales with the effective coupling constant $\frac{J}{W}$ and in the strong coupling *double exchange region*

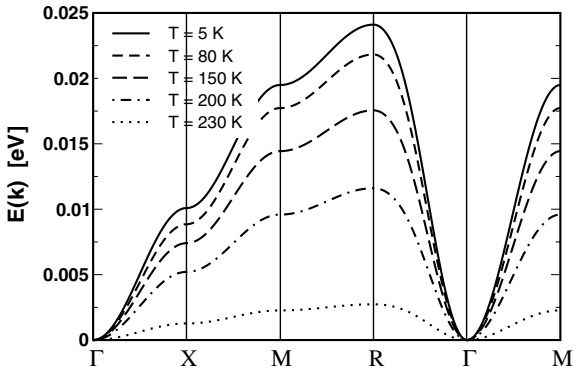

Figure 5. Spin-wave dispersion of the ferromagnetic Kondo-lattice model as a function of the wave vector for different temperatures T. Parameters: $J = 0.2$ eV, $n = 0.2$, $S = 7/2$, sc lattice and $W = 1$ eV. The self-consistently calculated Curie temperature is $T_C = 232$ K.

with the kinetic energy, i.e. $\propto W$. In figure 4(b) the change from RKKY behaviour (small $\frac{J}{W}$) to double exchange behaviour (large $\frac{J}{W}$) is clearly shown.

Figure 5 shows a typical example of a spin-wave dispersion, which obtains via the effective exchange integrals (12) a distinct temperature dependence. Upon heating the dispersion relation uniformly softens, disappearing above T_C. This agrees qualitatively with neutron scattering data on manganites [18].

4. Application to ferromagnetic EuO and EuS

In the last step we want to demonstrate how the model analysis can be used to describe real magnetic materials. We exemplify the method with respect to the classical local-moment ferromagnets EuO and EuS. These are ferromagnetic semiconductors which crystallize in the fcc-rocksalt structure with lattice constants $a = 5.142$ Å (EuO) and $a = 5.95$ Å (EuS), respectively. The physics of these materials is mainly determined by localized and half-filled 4f levels, on the one hand, and, on the other hand, by extended, at low temperature empty, 5d band states. In accordance with Hund's rule, the Eu^{2+}-4f shell produces a maximum spin moment $S = \frac{7}{2}$.

To investigate real materials such as EuO and EuS one has to exploit the multiband version of the KLM developed in section 1. As already explained, the hopping integrals $T_{ij}^{m\tilde{m}}$ in (1) have not only to incorporate the kinetic energy of the band electrons plus the influence of the periodic lattice potential but also as realistically as possible all those interactions which are not directly covered by the model Hamiltonian. For this purpose, we performed a band structure calculation based on density functional theory, using the Andersen scheme [19, 20] of a *tight binding linear muffin-tin orbital* (TB-LMTO) ansatz. LDA-typical difficulties arise with the strongly localized character of the 4f levels. A *normal* LDA calculation for EuO produces a metal with the 4f levels lying well within the conduction band. To circumvent the problem we considered the 4f electrons as core electrons, since our main interest is focused on the temperature reaction of the (empty) conduction bands. In our study the 4f levels appear only as localized spins (moments) in the sense of H_{ff} in equation (4). Figure 6 shows the so-derived spin-dependent band structure of EuS without the 4f levels. The low-energy part belongs to S-3p states, we are not interested in here, because only fd excitations shall be in the focus. The conduction band region is dominated by Eu-5d states, to which we have restricted the

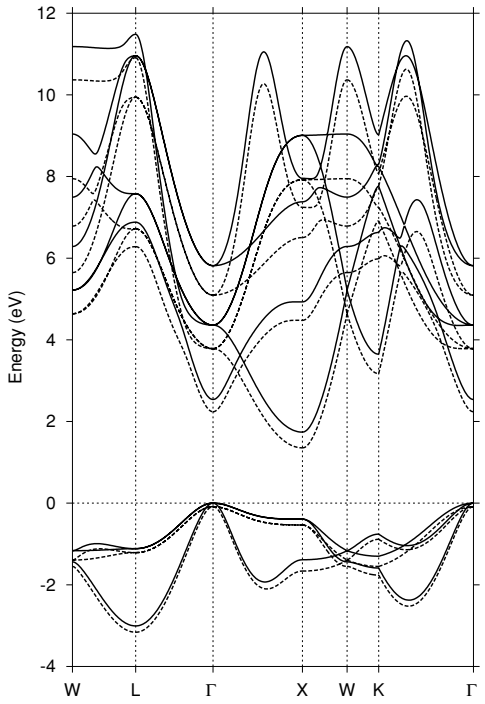

Figure 6. Spin-dependent (solid lines 'down-spin', broken lines 'up-spin') band structure of bulk EuS calculated within a TB-LMTO scheme with the 4f levels treated as core states. The energy zero coincides with the Fermi energy.

investigation by our combined many-particle, *first principles* procedure. For comparison, we have also performed an LDA+U calculation which indeed is able to put the respective bands into better positions. On the other hand, the results, which we are interested in, do not differ too strongly from those of LDA with the 4f electrons in the core. So we have chosen the much simpler LDA calculation, since our study mainly aims at overall correlation and temperature effects. The extreme details of the band structure are not so important.

The many-body treatment of the multiband KLM follows exactly the same line as for the single-band case, no need to create new approaches. However, we have to fix the only parameter of our procedure, the interband exchange J. It is generally assumed that an LDA treatment of ferromagnetism is quite compatible with a mean-field picture, so that the $T = 0$ shift of the $\uparrow$ and $\downarrow$ dispersions in figure 6 should amount to $\Delta = JS$. However, it can be seen that the assumption of a rigid shift is too simple. A certain energy dependence of the exchange splitting is found by LDA, too. We decided to use the splitting of the 5d band centre of gravity to fix the J for EuS at 0.23 eV [15]. Averaging over prominent features in the Q-DOS of EuO yields a similar value of $J = 0.25$ eV [16].

Another important issue concerns the renormalized single-particle input, because a double counting of the decisive interband exchange, once by the LDA input and once more explicitly in the model Hamiltonian (5), might produce rather misleading results. The most direct solution of this problem would be to switch off the interband exchange H_{df} in the LDA code, which turns out to be impossible. However, we can elegantly exploit the exact limiting case, discussed at the beginning of section 3. For zero temperature and zero band occupation the $\uparrow$ spectrum of the single as well as multiband KLM is only rigidly shifted towards lower energies

by the amount $\frac{1}{2}JS$. Thus we can use without any manipulation the ↑ dispersions of the LDA calculation ($T = 0$!) for the empty 5d bands as input for the single-electron Hamiltonian (1). There is no need to switch off H_{df} because in this special case it leads only to an unimportant rigid shift. Note that this holds only for the ↑ part, the ↓ spectrum is even at $T = 0$ strongly influenced by correlation effects (see figure 1). Therewith it is guaranteed, on the one hand, that all those interactions, which are not directly covered by the KLM, are implicitly taken into account by the LDA renormalized single-particle energies. On the other hand, a double counting of any decisive interaction, which usually occurs when combining first principles and many-body model calculations, is definitely avoided.

Because of the empty conduction bands a self-consistent justification of the EuO (EuS) ferromagnetism via the modified RKKY treatment of section 3 is not possible. The magnetic properties of the insulators EuO and EuS are exclusively due to the partial operator H_{ff} (4). Its exchange integrals between nearest (J_1) and next-nearest (J_2) neighbours have been derived by a neutron scattering spin-wave analysis [24]: $J_1/k_{\mathrm{B}} = 0.625\,(0.221)$ K, $J_2 = 0.125\,(-0.100)$ K for EuO (EuS). The single-ion anisotropy constant D does not play a decisive role as long as the bulk band structure and its temperature dependence are aimed at. However, when treating systems of lower dimensionality (films, surfaces) as done for EuO in [6, 21], then a finite D is necessary to overcome the Mermin–Wagner theorem [22] for getting a collective magnetic order of the moment system. D has been chosen in such a way that the experimental T_{C} value is correctly reproduced (see figure 3 in [15]). The temperature dependence of the 4f moment system leads to a remarkable induced temperature behaviour of the (unoccupied!) 5d spectrum. The evaluation of the effective Heisenberg model (4) is done by a Tyablikov decoupling of the equation of motion of a properly chosen spin Green function. Details are given in [11, 14].

Let us now select some typical results found for the archetypal ferromagnetic semiconductors EuO and EuS. We have no intention to be complete in this overview, rather to demonstrate the possibilities of our combined many-body/*ab initio* method. Figures 7 and 8 show the quasiparticle density of states (Q-DOS) for EuO and EuS, respectively, for five different 4f magnetizations, i.e. five different temperatures. Not surprisingly, the Q-DOS of EuO (figure 7) and EuS (figure 8) are qualitatively rather similar. Since we have taken into account the full band structure of the Eu-5d conduction bands, the symmetry of the different 5d orbitals is preserved. The 5d bands can therefore be decomposed into t_{2g} and e_g subbands, where the t_{2g} bands are substantially broader (~ 7 eV (EuS), ~ 9 eV (EuO)) than the e_g bands ($\sim$4 eV (EuS), $\sim$6 eV (EuO)). A remarkable temperature dependence shows up for both ferromagnets, manifesting itself, e.g., in a shift of the lower edge of the ↑ Q-DOS to lower energies upon cooling from $T = T_{\mathrm{C}}$ to $T = 0$. This explains the famous redshift of the optical absorption edge for the electronic 4f–$5d_{t_{2g}}$ transition, in the meantime observed for all ferromagnetic local-moment systems [23]. The temperature behaviour does not comply with the simple Stoner picture of an energy-independent induced exchange splitting of the spectra. The reason for the observed more complicated behaviour as a function of temperature is that in our theory correlation is treated in a way distinctly beyond mean-field.

While the Q-DOS refers to the spin resolved but angle averaged, direct or inverse photoemission experiment, the **k**-dependent spectral density is the angle resolved counterpart. Prominent peaks of the spectral density as a function of energy determine the $E(\mathbf{k})$ quasiparticle band structure (Q-BS). As an example, figure 9 represents the EuO-spectral density as a density plot for some symmetry directions and three different temperatures. The degree of blackening is a measure of the magnitude of the spectral density. For $T = 0$ ($\langle S_z \rangle = S$) the ↑-spectral density agrees, except for a constant shift, with the LDA result, being therefore a δ-function

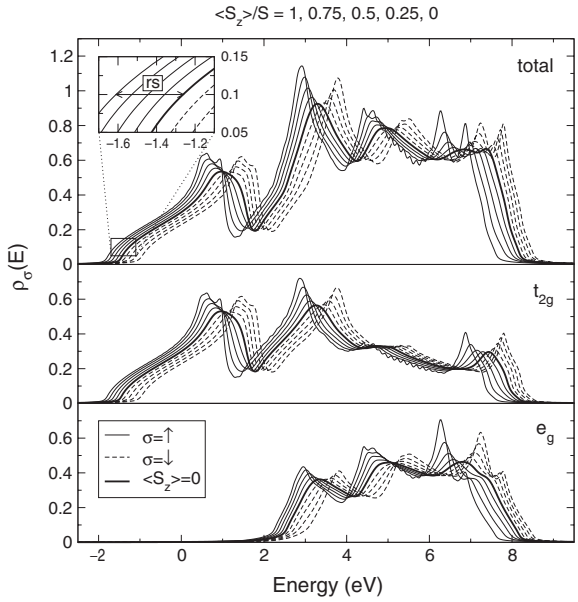

Figure 7. Temperature-dependent densities of states of the Eu-5d bands of bulk EuO ($J = 0.25$ eV). Solid lines: ↑ spectrum; broken lines: ↓ spectrum. Thick line: spectra for $T = T_C$ ($\langle S^z \rangle = 0$). The outermost curves belong to $T = 0$ ($\langle S^z \rangle = S$). With increasing temperature the ↑ and ↓ curves approach each other.

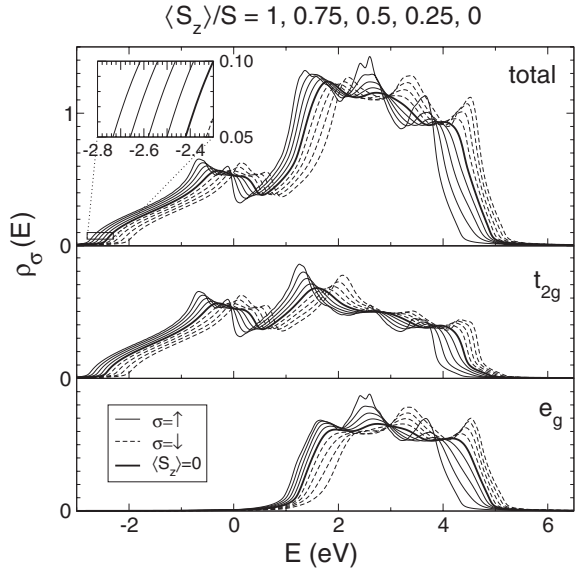

Figure 8. The same as in figure 7 but for bulk EuS ($J = 0.23$ eV).

at the excitation energy, corresponding to a quasiparticle with infinite lifetime. The ↓-spectral density, however, exhibits already at $T = 0$ a broadening of the dispersion curves, most notably around the Γ-point, which indicates finite quasiparticle lifetimes due to correlation effects. For intermediate temperatures ($\langle S_z \rangle = 0.5S$) a broadening sets in also for the ↑ dispersions

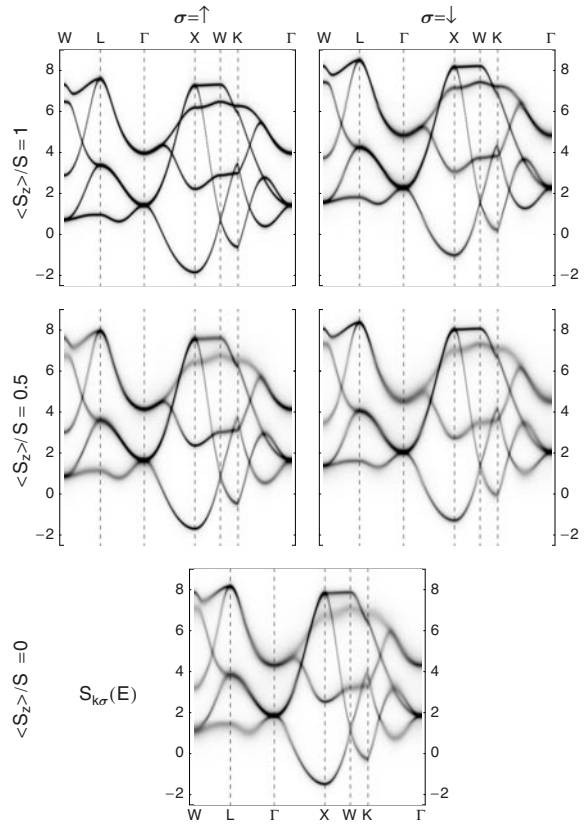

Figure 9. Spin-dependent quasiparticle band structure of the 5d bands of bulk EuO ($J = 0.25$ eV) for three different 4f magnetizations $\langle S^z \rangle$.

because the ↑ electron, too, can now exchange its spin with the no longer saturated local-moment system. In the ↓ spectrum correlation effects increase leading to further quasiparticle damping. Simultaneously, both spin spectra are shifted towards each other reducing therewith the effective exchange splitting. At $T = T_C$ ($\langle S_z \rangle = 0$) ↑ and ↓ dispersions coincide. Very similar behaviour is found for EuS [15].

As mentioned, the Q-BS has been derived from the spectral density. To give an insight into the temperature behaviour of the spectral density we have plotted in figure 10 for two **k**-points from the first Brillouin zone (Γ, W) the energy dependence of the spectral density for the same three 4f magnetizations as in figure 9, but now for EuS. For the Γ-point (figure 10(a)) we have to expect two structures according to the twofold degenerate (e_g) and threefold degenerate (t_{2g}) dispersions. Well-defined quasiparticle peaks appear, spin split below T_C. The spin splitting, induced via the interband coupling to the magnetically active 4f system, collapses for $T \to T_C$. One speaks of a *Stoner-type behaviour*. Quasiparticle damping, that scales with the peak width, obviously increases with temperature. At the W-point (figure 10 (b)) four sharp peaks show up in the ↑ spectrum, and, though already strongly damped, the same peak sequence appears in the ↓ part, too (compare with the Q-BS in figure 9). The reduction of the spin splitting with increasing temperature leads to a strong overlap of the two upper peaks, which are then no longer distinguishable. Altogether, the 5d spectral densities of the ferromagnetic semiconductors EuS and EuO (not shown here) exhibit drastic

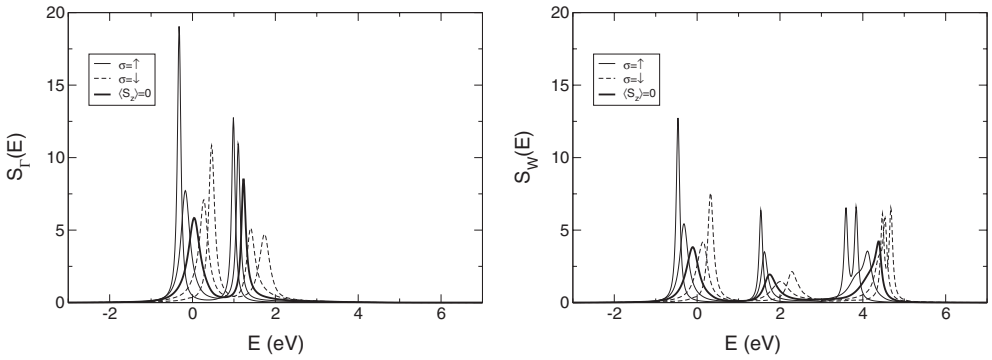

(*a*) (*b*)

Figure 10. (*a*) Spin-dependent spectral density $S_{\mathbf{k}\sigma}$ for $\mathbf{k}$ from the Γ-point (5d states) of bulk EuS ($J = 0.23$ eV) as a function of the energy for three different 4f magnetizations: $\langle S_z\rangle/S = 1.0, 0.5, 0$. Thick line for $T = T_C$. Solid lines: up-spin; broken lines: down-spin. Curves with maximum spin splitting of the peaks belong to $T = 0$. (*b*) The same as in (*a*) but for the *W*-point.

temperature dependences, that concern the positions and the widths of the quasiparticle peaks. The driving force is the interband (4f–5d) exchange interaction, the investigation of which was the main aim of the presented study.

5. Summary

We have demonstrated how the (multiband) Kondo-lattice model can be used for a realistic description of the strikingly temperature-dependent electronic excitation spectrum of local-moment ferromagnets. For this purpose we have combined a many-body evaluation of the KLM with a *first principles* band structure calculation (TB-LMTO) for the ferromagnetic semiconductors EuO and EuS.

In the first step we inspected an exactly solvable, non-trivial limiting case of the KLM to learn about the fundamental elementary excitations. In addition, this limiting case provides a weighty testing criterion for unavoidable approximations in the case of the not exactly solvable general case.

By using a self-consistent approach we found the electronic as well as magnetic properties of the KLM as functions of decisive model parameters such as band occupation and interband exchange coupling. By inspecting the Curie temperature we could demonstrate the transition from a weak-coupling RKKY behaviour to a strong-coupling double exchange scenario. It appears remarkable that both features are simultaneously involved in our theory.

Using a straightforward multiband version of the KLM with identical theoretical approaches we have worked out the influence of the localized magnetic 4f moments of the Eu^{2+} ion on the 5d conduction bands in EuO and EuS, respectively. The normally empty bands exhibit a distinct and unconventional (*'not Stoner-like'*) temperature-dependent exchange splitting induced by the interband exchange coupling to the 4f levels. As a special detail we observe the famous redshift effect in EuO as well as EuS.

Acknowledgment

Financial support by the SFB 290 of the Deutsche Forschungsgemeinschaft is gratefully acknowledged.

References

[1] Wachter P 1979 *Handbook of the Physics and Chemistry of Rare Earth* vol 1 (Amsterdam: North-Holland) ch 19
[2] Donath M, Dowben P and Nolting W (ed) 1998 *Magnetism and Electronic Correlations in Local-Moment Systems: Rare-Earth Elements and Compounds* (Singapore: World Scientific)
[3] Ohno H 1998 *Science* **281** 951
[4] Matsukara F, Ohno H, Shen A and Sugawara Y 1998 *Phys. Rev.* B **57** R2037
[5] Ramirez A P 1997 *J. Phys.: Condens. Matter* **9** 8171
[6] Schiller R, Müller W and Nolting W 2001 *Phys. Rev.* B **64** 134409
[7] Meyer D, Santos C and Nolting W 2001 *J. Phys.: Condens. Matter* **13** 2531
[8] Nolting W and Dubil U 1985 *Phys. Stat. Sol.* (b) **130** 561
[9] Nolting W, Dubil U and Matlak M 1985 *J. Phys.: Condens. Matter* **18** 3687
[10] Shastry B S and Mattis D C 1981 *Phys. Rev.* B **24** 5340
[11] Nolting W, Rex S and Mathi Jaya S 1997 *J. Phys.: Condens. Matter* **9** 1301
[12] Nolting W, Reddy G G, Ramakanth A and Meyer D 2001 *Phys. Rev.* B **64** 155109
[13] Nolting W, Reddy G G, Ramakanth A, Meyer D and Kienert J 2003 *Phys. Rev.* B **67** 024426
[14] Santos C and Nolting W 2002 *Phys. Rev.* B **65** 144419
[15] Müller W and Nolting W 2002 *Phys. Rev.* B **66** 085205
[16] Schiller R and Nolting W 2001 *Solid State Commun.* **118** 173
[17] Chattopadhyay A and Millis A J 2001 *Phys. Rev.* B **64** 024424
[18] Hwang H Y, Dai P, Cheong S W, Aeppli G, Tennant D A and Mook H A 1998 *Phys. Rev. Lett.* **80** 1316
[19] Andersen O K 1975 *Phys. Rev.* B **12** 3060
[20] Andersen O K and Jepsen O 1984 *Phys. Rev. Lett.* **53** 2571
[21] Schiller R and Nolting W 2001 *Phys. Rev. Lett.* **86** 3847
[22] Gelfert A and Nolting W 2001 *J. Phys.: Condens. Matter* **13** R505
[23] Batlogg B, Kaldis E, Schlegel A and Wachter P 1975 *Phys. Rev.* B **12** 3940
[24] Bohn H G, Zinn W, Dorner B and Kollmar A 1980 *Phys. Rev.* B **22** 5447